Composites Science and Technology 69 (2009) 2308–2314

Contents lists available at ScienceDirect

Composites Science and Technology

journal homepage: www.elsevier.com/locate/compscitech

Compression fatigue failure of CFRP laminates with impact damage

Nobuhide Uda [a,*], Kousei Ono [a], Kazuo Kunoo [b]

[a] Department of Aeronautics and Astronautics, Kyushu University, 744 Motooka, Nishi-ku, Fukuoka 819-0395, Japan
[b] Department of Aerospace Systems Engineering, Sojo University, 4-22-1 Ikeda, Kumamoto 860-0082, Japan

ARTICLE INFO

Article history:
Received 30 June 2008
Received in revised form 21 September 2008
Accepted 23 November 2008
Available online 10 December 2008

Keywords:
A. Polymer–matrix composites (PMCs)
B. Fatigue
Delamination
C. Damage tolerance
D. Ultrasonics

ABSTRACT

The objective of this study is to investigate failure mechanisms of impact-damaged CFRP laminates subjected to compression fatigue. Two kinds of composite materials, UT500/Epoxy and AS4/PEEK, were used to examine the dependence of failure behavior on the material properties such as interlaminar toughness. Impact-induced delaminations in the UT500/Epoxy specimen were considerably larger than those in the AS4/PEEK specimen. The *S–N* curves for the UT500/Epoxy specimens with impact damage exhibited a similar tendency to those without impact. The impact-induced delamination in the UT500/Epoxy specimen grew widthwise to the free edge on the rear side of the specimen during the fatigue test. On the other hand, the AS4/PEEK specimens without impact exhibited a more steeply declining *S–N* curve than those with impact damage. The delaminations in the impacted AS4/PEEK specimen did not reach the free edge before the fatigue fracture.

1. Introduction

The application of composite materials to aircraft primary structures is increasing due to their lightweight and high strength. However, the excellent mechanical properties of composite materials can be significantly reduced by a low velocity impact, such as tools dropped during maintenance and runway stones during taxiing. The compression-after-impact (CAI) strength of composite structures, in particular, is seriously reduced even if impact damage is not detectable by visual inspection. A number of investigations, e.g., [1–5] have been conducted to estimate the sensitivity of the CAI strength to low velocity impact damage. The fatigue behavior of impacted composite laminates has also been studied extensively during the past couple of decades, e.g., [6–14]. However, the effect of damage growth mechanisms on post-impact fatigue response has not been fully understood and an effective damage-tolerance methodology of post-impact composite laminates has not been established. The objective of this study is to investigate failure mechanisms of impact-damaged CFRP laminates subjected to compression fatigue. In this study, two kinds of composite materials were used to examine the dependence of failure behavior on the material properties such as interlaminar toughness. Some of the experimental observations obtained by post-impact compression fatigue tests are reported.

2. Experiments

2.1. Specimens

The composite systems used in these experiments were UT500/Epoxy (Toho Tenax, QU135-197A) and AS4/PEEK (ICI, APC-2). The AS4/PEEK laminate has a comparatively tougher interface than the UT500/Epoxy laminate. The critical strain energy release rates for mode-I fracture of these materials are 0.28 and 1.40 kJ/m^2, respectively. The lay-up sequence was $[+45/0/-45/90]_{ns}$; $n = 3$ for the UT500/Epoxy and $n = 4$ for the AS4/PEEK. The difference in the number of layups for each material gives almost the same nominal specimen thickness of 4 mm because the prepreg thicknesses are 0.19 mm for the UT500/Epoxy and 0.13 mm for the AS4/PEEK. Specimens that were 135 mm long and 50 mm wide were cut from 300 × 300 mm panels. In consideration of the loading capacity limit of 100 kN of the Instron 8501 fatigue testing machine, the width of the unimpacted specimens was reduced to 35 mm.

2.2. Impact tests

Impact tests were performed using a drop-weight test rig with an impactor having a 12 mm diameter hemispherical tup. The specimen was clamped between two plates, each with a 35 mm diameter circular window. The impactor was captured on the rebound after impact to prevent secondary strikes. The impactor velocity was measured using a laser displacement sensor. The impact energy was defined as the kinetic energy of the impactor just at the moment of first contact with the specimen. The impact energy is normalized by dividing by the thickness of the specimen.

* Corresponding author. Tel.: +81 92 802 3035; fax: +81 92 802 3001.
E-mail address: uda@aero.kyushu-u.ac.jp (N. Uda).

0266-3538/$ - see front matter © 2008 Elsevier Ltd. All rights reserved.
doi:10.1016/j.compscitech.2008.11.031

The normalized impact energy level was 0.5–2.0 J/mm in this study. The damage area induced by the impact load was tested using two ultrasonic C-scan systems based on the pulse-echo method, namely the Canon M-500A and GNES G-Scan 6AX500.

2.3. Static and fatigue tests

Static compression tests and compression fatigue tests were conducted in the servo-hydraulic testing machine with an end-loading fixture as shown in Fig. 1, which was built based on Shimokawa et al.'s study [15]. The specimen was placed in the fixture without tabs and was tightly clamped with binding grips. This fixture does not have an anti-buckling device as prescribed by ASTM D 695, but prevents an out-of-plane directional movement of the specimen by a pair of supporting guides for the whole of the fixture. The compression load is applied through end-sections of the specimen with the binding grips. A gage length of 35 mm for the compression specimen was selected to prevent global buckling of the unimpacted specimen at the initial stage of loading.

The compression–compression fatigue tests were conducted at 1 Hz with constant-amplitude sinusoidal loading, under ambient laboratory conditions. The maximum compressive stress of the cyclic loading was chosen to be 66–98% of the ultimate static strength, or the residual static strength for the impacted specimens. The minimum compressive stress during fatigue was fixed at 2.5 MPa for avoiding machine instabilities. Our experiments were intended to conduct the compression–compression fatigue tests with the stress ratio of $R = \infty$.

In some cases, monitoring of the damage progression during fatigue was performed periodically using the ultrasonic inspection systems to assess the change of the damaged area as a function of the number of load cycles. Some tests were interrupted prior to catastrophic failure so that the extent of the damage in the specimen could be inspected using a sectioning technique and microscopic examination.

3. Experimental results and discussion

3.1. Impact damage

The impact-induced damage was principally manifested in the form of delaminations. Fig. 2 shows the ultrasonic C-scan images of damage induced in a UT500/Epoxy specimen subjected to a 1.91 J/mm impact. The C-scan images in Fig. 2a and b were taken from the impacted side and the backside of the specimen, respectively, using the GNES G-Scan 6AX500 system. The depths of the delaminations are indicated using the color gradation shown at the top of Fig. 2. The delaminations are formed in a spiral-stair manner in the through-the-thickness direction with each step corresponding to a change in ply orientation. Therefore, the spiral direction is clockwise from the impacted side through the midplane and changes to counterclockwise below the midplane. The delamination size was measured by image processing. Fig. 3 shows the delamination size at each interface. In Fig. 3, the delamination size is represented as the diameter of a hypothetical circle on the assumption that the envelope of the damaged area was circular at each interface. The delamination size increased away from the impacted front face until the interface between the 19th 0-degree ply and the 20th +45-degree ply, and then decreased toward the backside, as shown in Figs. 2 and 3.

In the case of the AS4/PEEK specimen subjected to a 1.03 J/mm impact, the delamination area monotonically increased away from the impacted front face towards the back face. The three-dimensional envelope of the delaminations in the through-the-thickness direction created a truncated cone shape, as shown in Fig. 4 with the depth indicator using the color bar. The C-scan image in Fig. 4 was taken using the Canon M-500A system.

Ishikawa and Suemasu [1] introduced an effective diameter D_e for a unified description of CAI strength behavior obtained by various CAI test methods. The effective diameter D_e is defined as the average diameter of the hypothetical circle with equivalent area to the delamination geometry. We also adopt the parameter D_e normalized by the width b of the specimen to describe the size of the impact-induced delaminations.

Fig. 5 shows the relationships between the effective diameter of delaminations D_e and the normalized impact energy. Impacted specimens displayed a large scatter in the delamination diameter. The normalized effective diameter of delaminations of the UT500/Epoxy was relatively larger than that of the AS4/PEEK. This difference in observed damage extents may result from the difference between the fracture toughness values of the two material systems.

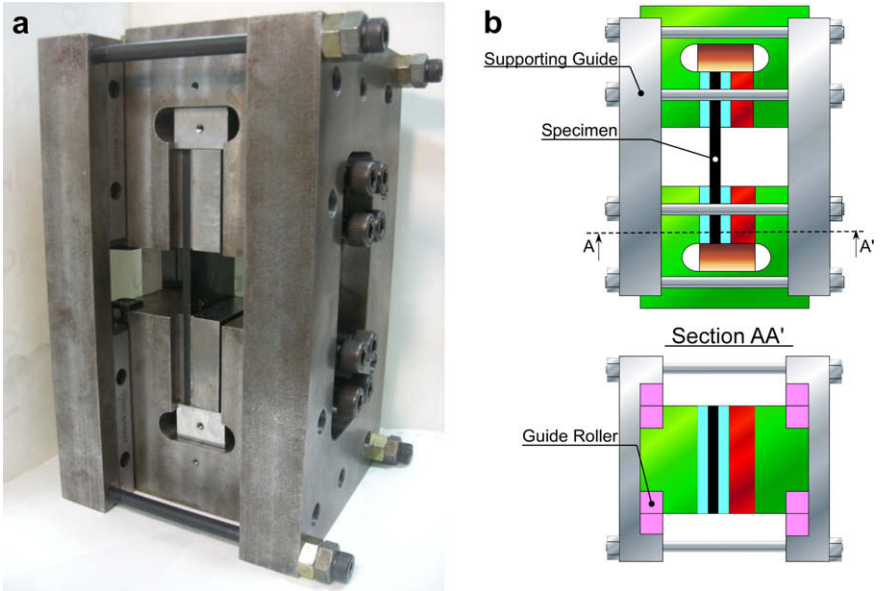

Fig. 1. Compression test fixture: (a) Actual and (b) schematic.